To further demonstrate that STAT1 is ubiquitinated upon phosphorylation in vivo, we prepared cell extracts at different times after treatment of HeLa cells with IFN-γ in the presence of MG132, which stabilizes the phosphorylated form of STAT1 (see Fig. 2). STAT1 proteins in prepared extracts (9) were then analyzed by immunoblot assays with anti-STAT1. High molecular weight forms of STAT1 were detected as phosphorylated STAT1 accumulated after stimulation with IFN-γ in the MG132-treated cells (Fig. 4A, lanes 4 and 5). These bands were not readily observed in extracts from HeLa cells treated with MG132 alone (lanes 2 and 3). Evidence that these high molecular weight bands correspond to ubiquitinated STAT1 was provided by the observation that they could be specifically recognized by antibody to ubiquitin (Fig. 4B). Thus, consistent with the data of Fig. 3, these results indicate that IFN-γ induces phosphorylation and ubiquitination of STAT1, and accumulation of ubiquitinated STAT1 in the presence of the proteasome inhibitor strongly suggests that activated STAT1 is degraded by the proteasome.

Phosphorylation of Tyr^{701} and Ser^{727} residues in STAT1 is induced by IFN-γ (*10*). We confirmed the importance of STAT1 phosphorylation in ubiquitination by testing the phosphorylation-defective double mutant of STAT1 (Y701F-S727A) in which Tyr^{701} and Ser^{727} were substituted by Phe^{701} and Ala^{727} in the in vivo ubiquitination assay (see Fig. 4A). U3A cells (*11*), which lack STAT1 protein, were transfected with expression plasmids for wild-type or mutant (Y701F-S727A) STAT1. The transfected cells were incubated with MG132 and then treated with IFN-γ. STAT1 and its tyrosine phosphorylation were detected by immunoblot analyses with anti-STAT1 and anti-phosphotyrosine, respectively (Fig. 4C). Ubiquitinated forms of STAT1 were readily detected in cells expressing wild-type STAT1 after treatment of both MG132 and IFN-γ (Fig. 4C, lane 8). In contrast, ubiquitination was greatly reduced in the cells treated with MG132 and IFN-γ that expressed the phosphorylation-defective STAT1 mutant (Fig. 4C, lane 12). Thus, phosphorylation of STAT1 is a prerequisite for its ubiquitination. Consistent with this conclusion, the tyrosine-phosphorylated form of STAT1 was ubiquitinated (Fig. 4C, bottom, lane 8). This regulatory mechanism is reminiscent of the phosphorylation-dependent degradation of G_1 cyclin (*12*) and of the NF-κB inhibitor IκBα (*9*, *13*).

On the basis of these observations, we propose that the amounts of phosphorylated STAT1 protein in IFN-γ–treated cells are, at least in part, controlled by ubiquitin-dependent proteolysis of STAT1. However, they do not rule out the possibility that the ubiquitin-proteasome pathway functions at other steps in the IFN-γ signal transduction pathway—for example, at the level of the IFN-γ receptor or kinase (*14*). It also is possible that the amount of activated STAT1 in the nucleus is controlled by dephosphorylation (*14*). These mechanisms are not mutually exclusive, because multiple control points may be required for stringent regulation of STAT activity.

REFERENCES AND NOTES

1. J. E. Darnell Jr., I. M. Kerr, G. R. Stark, *Science* **264**, 1415 (1994); J. N. Ihle, *Nature* **377**, 591 (1995); T. Taniguchi, *Science* **268**, 251 (1995).
2. K. Shuai, C. Schindler, V. R. Prezioso, J. E. Darnell Jr., *Science* **258**, 1808 (1992).
3. T. K. Kim and T. Maniatis, unpublished data.
4. V. J. Palombella, O. J. Rando, A. L. Goldberg, T. Maniatis, *Cell* **78**, 773 (1994); K. L. Rock *et al.*, *ibid.*, p. 761.
5. S. Jentsch, *Annu. Rev. Genet.* **26**, 177 (1992); A. Hersko and A. Ciechanover, *Annu. Rev. Biochem.* **61**, 761 (1992); A. Ciechanover, *Cell* **79**, 13 (1994); M. Hochstrasser, *Curr. Opin. Cell Biol.* **7**, 215 (1995); A. W. Murray, *Cell* **81**, 149 (1995); A. L. Goldberg, *Science* **268**, 522 (1995); R. J. Deshaies, *Trends Cell Biol.* **5**, 428 (1995).
6. M. Treier, L. M. Staszewski, D. Bohmann, *Cell* **78**, 787 (1994).
7. Cells were lysed in a buffer containing 6 M guanidinium hydrochloride, and ubiquitin-conjugated proteins were purified by nickel chromatography under the denatured condition. These denatured conditions significantly inhibit the deubiquitination activities. Otherwise, it is difficult to detect multi-ubiquitinated proteins because of potent isopeptidase activities that hydrolyze multi-ubiquitin chains.
8. N. Reich and L. M. Pfeffer, *Proc. Natl. Acad. Sci. U.S.A.* **87**, 8761 (1990).
9. Z. Chen *et al.*, *Genes Dev.* **9**, 1586 (1995). The extracts were prepared in the presence of SDS (0.1%) and *N*-ethylmaleimide (5 mM) to inhibit potent isopeptidase activities that may affect the detection of multi-ubiquitinated proteins.
10. K. Shuai, G. R. Stark, I. M. Kerr, J. E. Darnell Jr., *Science* **261**, 1744 (1993); Z. Wen, Z. Zhong, J. E. Darnell Jr., *Cell* **82**, 241 (1995).
11. M. Muller *et al.*, *EMBO J.* **12**, 4221 (1993).
12. M. Tyers, G. Tokiwa, R. Nash, B. Futcher, *ibid.* **11**, 1773 (1992); S. R. Salma, K. B. Hendricks, J. Thorner, *Mol. Cell. Biol.* **14**, 7953 (1994); R. J. Deshaies, V. Chau, M. Kirschner, *EMBO J.* **14**, 303 (1995); J. Yaglom *et al.*, *Mol. Cell. Biol.* **15**, 731 (1995).
13. S. Miyamoto, M. Maki, M. J. Schmitt, M. Hatanaka, I. Verma, *Proc. Natl. Acad. Sci. U.S.A.* **91**, 12740 (1994); K. Brown, S. Gerstberger, L. Carlson, G. Franzoso, U. Siebenlist, *Science* **267**, 1485 (1995); E. B.-M. Traenckner *et al.*, *EMBO J.* **14**, 2876 (1995).
14. R. L. Haspel, M. Salditt-Georgieff, J. E. Darnell Jr., *EMBO J.*, in press.

15. We thank G. Stark for the U3A cells, B. Ren and N. Pandey for comments on the manuscript, and J. E. Darnell for discussing unpublished results. Supported by the Cancer Research Fund of the Damon Runyon–Walter Winchell Foundation (DRG-1329 to T.K.K.) and NIH grant AI20642 (T.M.).

2 April 1996; accepted 29 July 1996

Regulation of a Neuronal Form of Focal Adhesion Kinase by Anandamide

Pascal Derkinderen, Madeleine Toutant, Ferran Burgaya, Marc Le Bert, Julio C. Siciliano,* Vittorio de Franciscis,† Michèle Gelman, Jean-Antoine Girault‡

Anandamide is an endogenous ligand for central cannabinoid receptors and is released after neuronal depolarization. Anandamide increased protein tyrosine phosphorylation in rat hippocampal slices and neurons in culture. The action of anandamide resulted from the inhibition of adenylyl cyclase and cyclic adenosine 3′,5′-monophosphate–dependent protein kinase. One of the proteins phosphorylated in response to anandamide was an isoform of pp125–focal adhesion kinase (FAK+) expressed preferentially in neurons. Focal adhesion kinase is a tyrosine kinase involved in the interactions between the integrins and actin-based cytoskeleton. Thus, anandamide may exert neurotrophic effects and play a role in synaptic plasticity.

Focal adhesion kinase (FAK) is a 125-kD cytosolic tyrosine kinase associated with focal adhesions in nonneuronal cells, where it is phosphorylated in response to integrin engagement and stimulation of various heterotrimeric GTP-binding protein (G protein)–coupled receptors (*1*). Autophosphorylated FAK recruits kinases of the Src family and triggers signaling cascades similar to those stimulated by growth factor receptors (*2*). In addition, FAK is enriched in brain, especially in hippocampus, and in young neurons, where it is located in growth cones (*3*). Phosphorylation of FAK is decreased in knockout mice deficient for the tyrosine kinase Fyn (*4*), which display abnormal hippocampal development and synaptic plas-

INSERM U 114, Chaire de Neuropharmacologie, Collège de France, 11 place Marcelin Berthelot, 75231 Paris cedex 05, France.

*Present address: Departamento de Histología, Facultad de Medicina, Montevideo, Uruguay.
†On leave of absence from Centro di Endocrinologia ed Oncologia Sperimentale del CNR, Università di Napoli "Federico II," Naples, Italy.
‡To whom correspondence should be addressed. E-mail: girault@infobiogen.fr

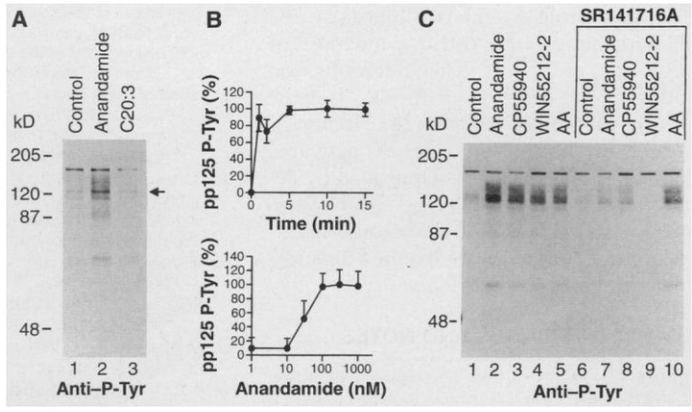

Fig. 1. Anandamide increases protein tyrosine phosphorylation in rat hippocampal slices by stimulation of cannabinoid CB1 receptors. (**A**) Rat hippocampal slices (*23*) were incubated in the absence (control, lane 1) or presence of either anandamide (1 μM, lane 2) or *N*-eicosatrienoyl ethanolamine (C20:3, 1 μM; lane 3) for 5 min. Slices were homogenized and proteins (40 μg per lane) were separated by electrophoresis (8% polyacrylamide) and transferred to nitrocellulose. Tyrosine phosphorylation was examined by antiphosphotyrosine (Anti–P-Tyr) immunoblotting with monoclonal antibody 4G10 (UBI) and chemiluminescence detection. (**B**) (Upper panel) Time course of the effects of anandamide (1 μM) on the main tyrosine-phosphorylated band (pp125, indicated by an arrow in Fig. 1A). A similar time course was observed for other responsive bands. Phosphorylation (P-Tyr) was quantified by densitometric measurement of autoradiograms. Data are expressed as a percentage of the maximal increase (mean ± SEM, $n = 3$). (Lower panel) Concentration-response curve of anandamide effects illustrated for the 125-kD band. Anandamide was applied for 5 min at the indicated concentrations (mean + SEM, $n = 4$ to 10). (**C**) Pharmacological characterization of anandamide effects on tyrosine phosphorylation in rat hippocampal slices. Slices were incubated for 5 min in the absence (control, lanes 1 and 6) or presence of either anandamide (1 μM, lanes 2 and 7), CP55940 (1 μM, lanes 3 and 8), WIN55212-2 (100 μM, lanes 4 and 9), or AA (1 μM, lanes 5 and 10). The slices were preincubated in the absence (lanes 1 to 5) or presence (lanes 6 to 10) of the specific CB1 antagonist SR141716A (50 μM, 50 min). The effects of anandamide, CP55940, and WIN55212-2, but not those of AA, were prevented by SR141716A.

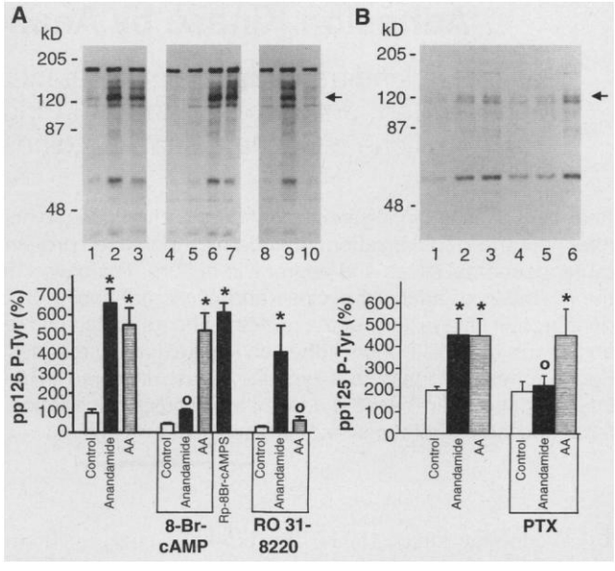

Fig. 2. Anandamide and AA increase tyrosine phosphorylation by distinct mechanisms. (**A**) Anandamide stimulated tyrosine phosphorylation by decreasing cAMP in rat hippocampal slices. Slices (*23*) were incubated for 5 min in the absence (control, lanes 1, 4, and 8) or presence of either anandamide (1 μM, lanes 2, 5, and 9) or AA (1 μM, lanes 3, 6, and 10). Pretreatment with 8-Br-cAMP (4 mM, applied 15 min before other drugs, lanes 4 to 6) prevented the effects of anandamide but not those of AA. Treatment of slices with the cell-permeant cAMP antagonist Rp-8Br-cAMPS (2 mM, 20 min, lane 7) increased protein tyrosine phosphorylation. Pretreatment of slices with a PKC inhibitor (50 μM RO 31-8220, 50 min, lanes 8 to 10) blocked the effects of AA but not those of anandamide. Quantified results for the main tyrosine-phosphorylated band (pp125, arrow) are indicated as a bar graph [mean + SEM, $n = 3$ to 10; statistical analysis by analysis of variance (ANOVA): $P < 10^{-6}$, followed by Fisher's least-significant-difference test: asterisk indicates different from controls, $P < 0.05$; circle indicates different from the effects in the absence of 8-Br-cAMP or RO 31-8220, $P < 0.05$]. (**B**) Rat forebrain neurons (*24*) were incubated in the absence (control, lanes 1 and 4) or presence of either anandamide (1 μM, lanes 2 and 5) or AA (1 μM, lanes 3 and 6) for 5 min. Anandamide and AA increased protein tyrosine phosphorylation. Pretreatment of cultures with pertussis toxin (PTX, 200 ng/ml for 18 hours, lanes 4 to 6) prevented the effects of anandamide but not those of AA. Quantified results for pp125 (arrow) are indicated as a bar graph (mean + SEM, $n = 7$; ANOVA: $P < 10^{-6}$; Fisher's test: asterisk indicates different from controls, $P < 0.05$; circle indicates different from the effects in the absence of PTX, $P < 0.05$).

ticity (*5*). Inhibitors of tyrosine kinases also impair synaptic plasticity (*6*). Although several neurotransmitters have been shown to stimulate tyrosine phosphorylation pathways (*7*, *8*), the function and regulation of FAK in neurons are not known. We investigated the effects of anandamide, an endogenous ligand for central cannabinoid CB1 receptors (*9*), which are highly enriched in the hippocampus (*10*).

Treatment of rat hippocampal slices with anandamide [(1 μM *N*-arachidonoyl ethanolamine (C20:4)] for 5 min increased tyrosine phosphorylation of several proteins including components of 60, 110, and 125 kD (Fig. 1A). The specificity of anandamide was shown by the lack of effect of two analogs in which the *N*-arachidonoyl moiety was replaced by fatty acid chains of identical length but with a decreased number of double bonds [C20:3 (Fig. 1A) and C20:1 (*11*)]. The effect of anandamide was rapid (Fig. 1B) and was observed at concentrations compatible with the stimulation of cannabinoid CB1 receptors [median effective concentration (EC_{50}) ~30 nM] (Fig. 1B). Pharmacological characterization lent further support to this possibility. First, two chemically unrelated CB1 agonists, CP55940 and WIN55212-2 (*12*), mimicked the stimulatory effects of anandamide on protein tyrosine phosphorylation (Fig. 1C). Second, SR141716A, a selective antagonist of CB1 receptors (*13*), blocked completely the effects of anandamide, WIN55212-2, and CP55940 (Fig. 1C).

CB1 receptors are negatively coupled to adenylyl cyclase via a G_i protein (*12*). To test whether decreased concentrations of adenosine 3′,5′-monophosphate (cAMP) were responsible for the effects of anandamide, we used cell-permeant analogs of cAMP. The effects of anandamide on tyrosine phosphorylation were prevented by pretreatment of slices with 8-Br-cAMP, which stimulates cAMP-dependent protein kinase (PKA) (Fig. 2A). Conversely, treatment of slices with two unrelated inhibitors of PKA, Rp-8Br-cAMPS (Fig. 2A) or H8 (*11*), mimicked the effects of anandamide on tyrosine phosphorylation. Thus, anandamide relieved a tonic inhibition exerted by basal concentrations of cAMP on tyrosine phosphorylation in hippocampal slices.

Anandamide may generate arachidonic acid (AA) either as a product of its own hydrolysis by endogenous anandamide hydrolases (*14*) or by stimulation of phospholipase A2 (*15*). We examined the effects of AA (1 μM) on protein tyrosine phosphorylation in rat hippocampal slices and found that they were similar to those of anandamide but, as expected, were not blocked by SR141716A (Fig. 1C). However, further analysis showed that AA was unlikely to

mediate the effects of anandamide because the mechanisms of action of these two compounds on tyrosine phosphorylation were different: the effects of AA were insensitive to 8Br-cAMP but were fully blocked by RO 31-8220, a protein kinase C (PKC) inhibitor, which had no significant effect on anandamide action (Fig. 2A). Thus, AA stimulated protein tyrosine phosphorylation through activation of PKC, a mechanism similar to that reported for several neurotransmitters (*7*, *8*) but different from that used by anandamide.

To identify the cell type on which anandamide and AA were active, we used primary cultures of embryonic forebrain cells, highly enriched in either neurons or astrocytes (*16*). Although their effects were less pronounced than in slices, anandamide and AA stimulated protein tyrosine phosphorylation in neurons (Fig. 2B), whereas they had no effect in astrocytes (*11*). The pharmacological profile of anandamide was similar to that observed in slices, except that WIN55212-2 and SR141716A were active at lower concentrations (*11*), probably as a result of the better accessibility of neurons in culture to these drugs. In addition, pretreatment of neurons with pertussis toxin, which selectively inactivates $G_{\alpha i}$ and $G_{\alpha o}$, prevented the effects of anandamide but not those of AA (Fig. 2B).

The 125-kD protein phosphorylated in response to anandamide or AA comigrated with FAK (Fig. 3A). Immunoprecipitation with serum SL38 showed that anandamide and AA increased FAK tyrosine phosphorylation in hippocampal slices (Fig. 3B), as well as in neurons in culture (*11*). Thus, FAK was one of the 120- to 130-kD proteins for which phosphorylation was stimulated in response to these agents. However, phosphorylation of PYK2 or Cakβ, a 110-kD tyrosine kinase closely related to FAK and enriched in neurons (*17*), was unaltered after treatment of hippocampal slices with anandamide or AA (*11*), indicating a difference in the regulation of these two kinases. Pretreatment of slices with 8Br-cAMP prevented the effect of anandamide but not that of AA on FAK phosphorylation (Fig. 3C). Conversely, PKA inhibitors (Rp-8Br-cAMPS and H8) increased FAK phosphorylation by themselves (Fig. 3C), supporting the importance of cAMP and PKA in the regulation of FAK tyrosine phosphorylation.

The FAK sequence is highly conserved in vertebrates but is encoded by several different mRNAs that presumably are generated by alternative splicing of the same gene product (*18*, *19*). One of these variants, called FAK+, contains an insertion of three amino acids in the focal adhesion targeting region (FAT in Fig. 4A), the mRNA of which is preferentially expressed

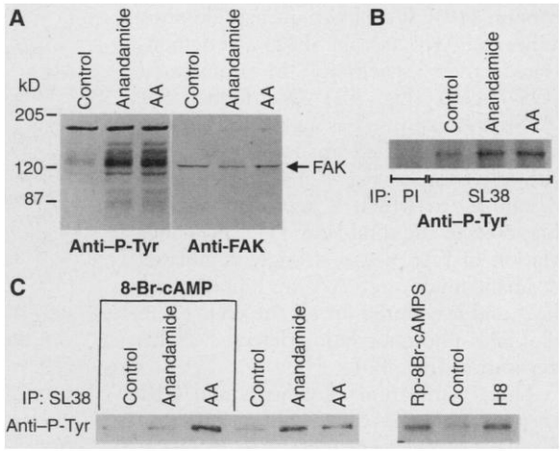

Fig. 3. Anandamide and AA increase tyrosine phosphorylation of FAK in rat hippocampal slices. (**A**) The 125-kD tyrosine-phosphorylated band comigrated with FAK. Homogenates from hippocampal slices incubated for 5 min in the absence (control) or presence of either anandamide (1 μM) or AA (1 μM) were analyzed by Anti–P-Tyr immunoblotting. Antibodies were eluted and the membrane reprobed with monoclonal antibody to FAK (2A7, UBI) (Anti-FAK). Levels of FAK were unaffected by the treatments. (**B**) Immunoprecipitation (IP) (*25*) of FAK from hippocampal slices incubated for 5 min in the absence (control) or presence of either anandamide (1 μM) or AA (1 μM) was carried out with rabbit preimmune serum (PI) or antiserum against FAK (SL38). Analysis of the immunoprecipitates by Anti–P-Tyr immunoblotting showed that anandamide and AA increased tyrosine phosphorylation of FAK. The level of FAK, estimated with an in vitro phosphorylation assay, was the same in each immunoprecipitate (*11*). (**C**) The effects on FAK phosphorylation of anandamide (1 μM, 5 min), but not those of AA (1 μM, 5 min), were prevented by 8-Br-cAMP (4 mM, 20 min) and mimicked by the PKA inhibitors Rp-8Br-cAMPS (1 mM, 20 min) and H8 (100 μM, 20 min). FAK was immunoprecipitated from hippocampal slices with antiserum SL38 and tyrosine phosphorylation was detected by immunoblotting. Data presented are representative of experiments carried out at least three times with similar results.

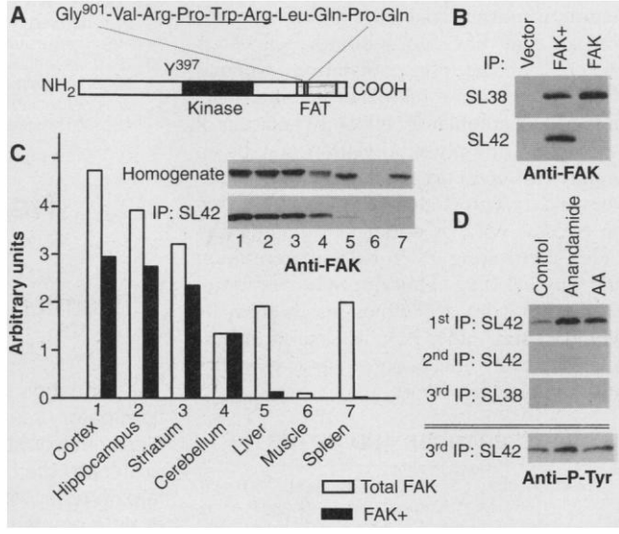

Fig. 4. Anandamide and AA increase tyrosine phosphorylation of FAK+, a variant of FAK expressed preferentially in neurons. (**A**) The sequence of FAK+ is characterized by the insertion of three aminoacyl residues [underlined (*19*)] in the FAT (*26*). A rabbit antiserum (SL42) was raised against a peptide encompassing this insertion. The sequence of this peptide and the positions of the autophosphorylated tyrosine (Y^{397}) and of the kinase domain are indicated. (**B**) COS-7 cells were transfected with CMV2 plasmid vector or with the same plasmid with an insert encoding rat FAK+ (including the three–amino acid insertion) or FAK [without this insertion (*27*)]. IPs were carried out with SL38 or SL42 (*25*) and the precipitates analyzed by immunoblotting with monoclonal 2A7, which reacts equally well with both forms of FAK. SL42 immunoprecipitated FAK+ but not FAK without the insertion, whereas SL38 immunoprecipitated both forms. (**C**) The distribution of total FAK and of FAK+ was studied in various rat tissues by immunoblotting with monoclonal 2A7 of either total homogenate (upper lane) or after immunoprecipitation with SL42 (lower lane). Quantification of the results from duplicate experiments is shown as a bar graph: the amount of total FAK was estimated by immunoblotting of the homogenate and the amount of FAK+, expressed in the same arbitrary units, was calculated by immunoblotting of immunoprecipitates by SL42 and by SL38 (not shown) corrected for the yield of immunoprecipitation. (**D**) FAK+ phosphorylation accounted for all the changes in FAK phosphorylation in hippocampal slices. Slices were incubated for 5 min in the absence (control) or presence of either anandamide (1 μM) or AA (1 μM). Homogenates were subjected to sequential IPs and analyzed by Anti–P-Tyr immunoblotting. The first IP with the antibody specific for FAK+ (SL42) showed that FAK+ was phosphorylated in response to anandamide and AA. IP of the resulting supernatants with the same antibody and then with antibody to total FAK (SL38) did not precipitate additional phosphorylated FAK, demonstrating that all the phosphorylated FAK in response to anandamide or AA was FAK+. As a control and to rule out dephosphorylation of FAK during the experiment, IP with SL42 was also carried out after the two other IPs with an irrelevant antibody (3^{rd} IP: SL42).

in brain (*19*). We raised antipeptide antibodies to FAK+ (serum SL42) and demonstrated their specificity in transfected COS-7 cells (Fig. 4B). We found that FAK+ was expressed as a protein that was particularly enriched in brain compared with other tissues (Fig. 4C), and in neurons in culture, in which it represented more than 80% of the total FAK (*11*). Phosphorylation of FAK+ was strongly stimulated by anandamide and AA in hippocampal slices and accounted for all the changes in total FAK phosphorylation detected in this preparation (Fig. 4D).

Thus, stimulation of cannabinoid CB1 receptors increased tyrosine phosphorylation of several proteins including FAK+ by inhibiting adenylyl cyclase and PKA. The mechanism by which PKA regulates tyrosine phosphorylation is not known; it may involve inhibition of a tyrosine kinase or, as proposed in *Aplysia* neurons (*20*), stimulation of a tyrosine phosphatase. The effects of anandamide differed from those of AA and from those of neurotransmitters, including norepinephrine, acetylcholine, and glutamate (*7*, *8*), which involve PKC. Therefore, neurotransmitters that raise cAMP concentrations may have an inhibitory effect on protein tyrosine phosphorylation, whereas those that decrease cAMP or activate PKC may have a stimulatory effect. Regulation of FAK+ tyrosine phosphorylation may be an important step in the regulation of ion channels and receptors that are phosphorylated on tyrosine (*21*), as well as of signaling cascades controlling neuronal differentiation and survival (*22*). Thus, phosphorylation of FAK+ provides a common mechanism by which anandamide, AA, or neurotransmitters may exert effects on synaptic plasticity and neuronal trophicity.

REFERENCES AND NOTES

1. M. D. Schaller, J. T. Parsons, *Curr. Opin. Cell Biol.* **6**, 705 (1994); M. A. Schwartz, M. D. Schaller, M. H. Ginsberg, *Annu. Rev. Cell. Dev. Biol.* **11**, 549 (1995).
2. D. D. Schlaepfer, S. K. Hanks, T. Hunter, P. Van der Geer, *Nature* **372**, 786 (1994); H.-C. Chen and J.-L. Guan, *Proc. Natl. Acad. Sci. U.S.A.* **91**, 10148 (1994); C. Guinebault *et al.*, *J. Cell Biol.* **129**, 831 (1995).
3. F. Burgaya, A. Menegon, M. Menegoz, F. Valtorta, J.-A. Girault, *Eur. J. Neurosci.* **7**, 1810 (1995).
4. S. G. N. Grant, K. A. Karl, M. A. Kiebler, E. R. Kandel, *Genes Dev.* **9**, 1909 (1995).
5. S. G. N. Grant *et al.*, *Science* **258**, 1903 (1992).
6. T. J. O'Dell, E. R. Kandel, S. G. N. Grant, *Nature* **353**, 558 (1991); A. R. Boxall, B. Lancaster, J. Garthwaite, *Neuron* **16**, 805 (1996).
7. X.-Y. Huang, A. D. Morielli, E. G. Peralta, *Cell* **75**, 1145 (1993).
8. J. C. Siciliano, M. Gelman, J.-A. Girault, *J. Neurochem.* **62**, 950 (1994).
9. W. A. Devane *et al.*, *Science* **258**, 1946 (1992); V. Di Marzo *et al.*, *Nature* **372**, 686 (1994).
10. L. A. Matsuda, S. J. Lolait, M. J. Brownstein, A. C. Young, T. I. Bonner, *Nature* **346**, 561 (1990).
11. P. Derkinderen, M. Toutant, M. Gelman, J.-A. Girault, unpublished observations.
12. A. C. Howlett, *Annu. Rev. Pharmacol. Toxicol.* **35**, 607 (1995).
13. M. Rinaldi-Carmona *et al.*, *FEBS Lett.* **350**, 240 (1994).
14. F. Desarnaud, H. Cadas, D. Piomelli, *J. Biol. Chem.* **270**, 6030 (1995).
15. M. Wartmann, D. Campbell, A. Subramanian, S. H. Burstein, R. J. Davis, *FEBS Lett.* **359**, 133 (1995).
16. B. Chamak, A. Fellous, J. Glowinski, A. Prochiantz, *J. Neurosci.* **7**, 3163 (1987).
17. S. Lev *et al.*, *Nature* **376**, 737 (1995); H. Sasaki *et al.*, *J. Biol. Chem.* **270**, 21206 (1995).
18. M. D. Schaller, C. A. Borgman, J. T. Parsons, *Mol. Cell. Biol.* **13**, 785 (1993).
19. F. Burgaya and J.-A. Girault, *Mol. Brain Res.* **37**, 63 (1996).
20. G. F. Wilson and L. K. Kaczmarek, *Nature* **366**, 433 (1993).
21. J. F. Hopfield, D. W. Tank, P. Greengard, R. L. Huganir, *ibid.* **336**, 677 (1988); Y. T. Wang and M. W. Salter, *ibid.* **369**, 233 (1994); S. J. Moss, G. H. Gorrie, A. Amato, T. G. Smart, *ibid.* **377**, 344 (1995); M. Menegoz, L. F. Lau, D. Hervé, R. L. Huganir, J.-A. Girault, *Neuroreport* **7**, 125 (1995).
22. S. Finkbeiner and M. E. Greenberg, *Neuron* **16**, 233 (1996).
23. Rat hippocampal slices (300 μm) were prepared from male Sprague-Dawley rats (100 to 150 g) as described (*8*) and incubated (three slices per tube) at 35°C for 50 min before pharmacological treatments. At the end of the experiment, slices were sonicated in a solution of SDS (200 μl, 1% w/v) and sodium orthovanadate (1 mM) in water at 100°C, placed in a boiling water bath for 5 min, and stored at −20°C until biochemical analysis.
24. Neurons, prepared from 17-day-old rat embryos, were cultured in a monolayer in serum-free conditions (*16*). Thirty minutes before drug application, the medium was replaced with artificial cerebrospinal fluid (*8*). After treatment, the fluid was aspirated and the cells were solubilized in 1% (v/v) Triton X-100, deoxycholate (1 mg/ml), SDS (1 mg/ml), 158 mM NaCl, 10 mM tris-HCl (pH 7.2), 1 mM sodium orthovanadate, 1 mM 4-(2-aminoethyl)-benzenesulfonyl fluoride, and pepstatin A, leupeptin, and trasylol (50 μg/ml each).
25. For immunoprecipitation, six hippocampal slices were homogenized in ice-cold buffer [100 mM NaCl, 50 mM tris-HCl (pH 7.4), 5 mM EDTA, and 50 mM NaF] containing 1 mM Na^+ orthovanadate, 1% (v/v) NP-40, and protease inhibitors (Complete, Boehringer). Immunoprecipitation was carried out with 20 μl of either preimmune serum or rabbit antisera SL38, or SL42 preadsorbed on protein A–Sepharose beads. SL38 was prepared by immunizing a rabbit against the NH_2-terminal fragment of rat FAK [residues 1 to 377 (*19*)] expressed in *Escherichia coli* as a hexahistidine fusion protein. SL42 was raised against a peptide (Fig. 4A) coupled to keyhole limpet hemocyanin.
26. J. D. Hildebrand, M. D. Schaller, J. T. Parsons, *J. Cell Biol.* **123**, 993 (1993).
27. The plasmid used for transfection, pCMV2, was derived from pBK-CMV (Stratagene) by deletion of an Nhe I–Sal I fragment corresponding to the bacterial promoter. pCMV2-C^+19 and pCMV2-C^-19 contained inserts corresponding to rat FAK cDNA with (FAK+) or without (FAK) the insertion coding for the three amino acids Pro-Trp-Arg (*19*). COS-7 cells were transfected in the presence of *N*-[1-(2,3-dioleoyl)propyl]-*N*,*N*,*N*-trimethylammonium methyl sulfate (DOTAP, Boehringer) according to the manufacturer's instructions. Cells were lysed 72 hours after transfection.

28. C. Giaume and J. Glowinski are gratefully acknowledged for critical reading of the manuscript. F.B. was supported by the European Commission Human Capital and Mobility Programme (CT940705), J.C.S. by ECOS (Comité: Evaluation orientation de la Coopération Scientifique) and the European Commission International Scientific Cooperation (CT940038), V.deF. by INSERM, and M.L.B. by Association Française contre les Myopathies.

6 June 1996; accepted 19 July 1996

Neurogenic Amplification of Immune Complex Inflammation

Carmen R. Bozic,* Bao Lu,* Uta E. Höpken, Craig Gerard, Norma P. Gerard†

The formation of intrapulmonary immune complexes in mice generates a vigorous inflammatory response characterized by microvascular permeability and polymorphonuclear neutrophil influx. Gene-targeted disruption of the substance P receptor (NK-1R) protected the lung from immune complex injury, as did disruption of the C5a anaphylatoxin receptor. Immunoreactive substance P was measurable in fluids lining the lung at time points before neutrophil influx and may thus be involved in an early step in the inflammatory response to immune complexes in the lung.

Immune complexes underlie the inflammatory response seen in a variety of rheumatologic illnesses, including arthritis, vasculitides, and systemic lupus erythematosus (*1*). Antigen-antibody aggregates may be deposited locally and incite edema through enhanced microvascular permeability to plasma proteins as well as elicit exudates of acute inflammatory leukocytes typified by the polymorphonuclear neutrophil (PMN). The mechanisms of injury induced by the immune complex are modeled in experimental animals by the Arthus reaction, in which specific antibody and antigen are passively introduced across a vascular barrier (*2*). Studies on rabbit skin and in mice deficient in complement component C5 implicated complement proteins as crucial participants in the inflammatory response (*3*), a role that has been reinvestigated through the use of mast cell and Fc receptor–deficient mice (*4*). We now use strains of mice deficient in the receptors for sub-

Perlmutter Laboratory, Children's Hospital, 300 Longwood Avenue, Boston, MA 02115, USA.

*These authors contributed equally to this work.
†To whom correspondence should be addressed.